Physics of the Earth and Planetary Interiors 242 (2015) 9–23

Contents lists available at ScienceDirect

Physics of the Earth and Planetary Interiors

journal homepage: www.elsevier.com/locate/pepi

Using "domino" model to study the secular variation of the geomagnetic dipolar moment

B. Duka [a,*], K. Peqini [a], A. De Santis [b], F.J. Pavón-Carrasco [b]

[a] Dept. of Physics, Faculty of Natural Sciences – University of Tirana, Albania
[b] Istituto Nazionale di Geofisica e Vulcanologia, Roma, Italy

ARTICLE INFO

Article history:
Received 23 July 2014
Received in revised form 20 February 2015
Accepted 4 March 2015
Available online 14 March 2015

Keywords:
Geomagnetic reversal
Geomagnetic excursion
Domino model
Secular variation
Dipolar magnetic moment
Geodynamo

ABSTRACT

Aiming to understand the physical processes underneath the reversals events of geomagnetic field, different numerical models have been conceived. We considered here the so named "domino" model, an Ising–Heisenberg model of interacting magnetic macrospins aligned along a ring. This model was proposed by Mazaud and Laj (1989) and then applied by Mori et al. (2013) to study geomagnetic field reversals.

The long series of the axial magnetic moment (dipolar moment or "magnetization") generated by the "domino" model are empirically studied by varying all model parameters. We present here some results which are slightly different from those given by Mori et al. (2013), and will provide our explanation on the presence of these differences. We also define the set of parameters that supply the longest mean time between reversals. Using this set of parameters, a large number of time series of axial magnetic moment are also generated. After de-noising the fluctuation of these time series and averaging them, we compared the resulting averaged series with the series of axial dipolar magnetic moment values supplied by CALS7k.2, and CALS10k.1b models, finding similar behavior for the all time series. In a similar way, we also compared the averaged 14,000 years long series of dipolar moment with the dipolar magnetic moment obtained by the model SHA.DIF.14k.

1. Introduction

At the present, the physical mechanisms in the liquid outer core that generate and maintain the geomagnetic main field are mostly known. Although inside the core it is expected that the geomagnetic field possesses a variety of complex patterns, when it is observed at the Earth's surface it is mostly a dipolar field. However the mechanisms responsible for the remarkable features of the time variations of the main geomagnetic field are not yet completely known.

Time changes in the dipole moment occur on a wide timescales: in general, changes at shorter timescales ($1 \div 10^3$ years) are small and are classified as secular variation (SV), while the greatest variations at longer periods (>10^3 years) are those associated with excursions or with full reversals of the geomagnetic field.

The switch between the two preferred macroscopic states of the Earth's magnetic field, the reverse and the normal polarities, is commonly referred to as a polarity reversal (Glaßmeier et al., 2009). According to Merrill et al. (1996), a geomagnetic reversal is defined as a "globally observed 180° change in the dipole field averaged over a few thousand years". Paleomagnetic data shows that reversals occurred many times during Earth's history at irregular intervals (Jacobs, 1994; Merrill et al., 1996). Although the rate at which reversals occur is not uniformly well-determined, it is nevertheless clear that the rate has varied throughout geological time. Examination of the reversal history suggests that reversals occur at apparently random intervals without a predictable pattern (e.g. Fig. 7a). The time periods of the same direction of dipole orientation, named *chrons*, varies by nearly three orders of magnitude, i.e. from 40 Myr long superchrons (e.g. CNS – Cretaceous Normal Superchron) to short subchrons lasting even less than 40 kyr (Cande and Kent, 1995; Merrill et al., 1996). According to paleomagnetic data, the mean chron duration depends on the total time period, i.e. the reversals happened every about 300 kyr for the last 5 million years, every about 400 kyr for the last 83 Myr (not including the duration of CNS; e.g. De Santis et al., 2013), every about 500 kyr for the last 166 Myr. Such different estimations are probably due to the increasing of inaccuracy by enlarging the geological time and to the presence of CNS

* Corresponding author at: Dept. of Physics, Faculty of Natural Sciences – University of Tirana, Bulevardi Zogu I, Nr. 25, Tirana, Albania. Mobile: +355 692608193.
E-mail address: bejo.duka@unitir.edu.al (B. Duka).

http://dx.doi.org/10.1016/j.pepi.2015.03.001
0031-9201/

macrochron. Most reversals inverted their polarity in a time (called reversal time) between 100 and 10,000 years (Merrill et al., 1996), although the question is still under debate (Sagnotti et al., 2014).

One can find among the paleomagnetism community different definitions of excursions (e.g., Roberts, 2008). Usually, excursions are defined as periods during which the geomagnetic pole deviates from geographic pole beyond the "normal" range of secular variation (Constable, 2001). The threshold of the geomagnetic pole deviation is varied according to different authors: for example by more than 40° away from the geographic pole (Valet et al., 2008), or more than 45° (Verosub, 1977). While other authors apply different criteria to distinguish the excursions, for example by means of "an adaptive cutoff angle" method (Vandamme, 1994). A widespread interpretation of excursions is as aborted reversals in which the field returns to its original state after a large perturbation.

Reversals and excursions occur generally during periods of very weak dipole field intensity (Guyodo and Valet, 1999) and could thus well be associated with similar magnetic processes within the outer terrestrial core leading to either successful or aborted reversals depending on the conditions that could be related to the influence of the inner core (Gubbins, 1999). Alternately, excursions can be regarded as secular variation events of large amplitude, in contrast to reversals which are sometimes assigned longer duration and larger spatial scales (Lund et al., 2006).

Numerical simulations of the geodynamo (e.g. Glatzmaier and Roberts, 1995, 1997) demonstrated several inversions proving that magneto-hydrodynamic differential partial equations are satisfied by both the orientations of the field regarding the Earth rotation axis, but not revealing the cause of the reversals (Amit et al., 2010). Most numerical simulations of the geodynamo successfully reproduced many features of the magnetic field of the Earth, including stochastic reversals (Christensen and Wicht, 2007). Numerical dynamo studies in particular have also identified several factors such as the vigor of convection, the rate of rotation, the heterogeneous core–mantle boundary (CMB) heat flux, that control the likelihood of reversals (Olson and Amit, 2014).

Modern numerical simulations make it possible the generation of numerical sequences of magnetic polarity reversals over periods of time equivalent to several tens of millions of years. For example, Lhuillier and Gilder (2013) numerically integrated over equivalent to 40–50 Myr, so generating synthetic data analogous to paleomagnetic data derived from volcanic flows and they found that the distributions of directions are remarkably similar to those observed in the paleomagnetic database. Their results suggest that reversals and excursions may not be extraordinary events but part and parcel of paleosecular variation as proposed by Biggin et al. (2008) for the geomagnetic field. In other words, this implies a continuum among paleosecular variation, reversals and excursions. In order to detect reversals, "failed" reversals and "stable low intensity" events in the dynamo solutions, Lhuillier et al. (2013) estimated the mean μ over the whole dynamo numerical solution of the axial dipole moment (ADM) and its standard deviation σ and determined time intervals Δt of "low intensity" during which the ADM is lower than $\mu - \sigma$. According to them a reversal is identified if the Dipole Pole is in different hemisphere at extremities of the time interval Δt, a failed reversal is identified if the Dipole Pole is in the same hemisphere at the extremities of Δt.

In order to count only "true" reversals (not "false" reversals and excursions) in the long magnetization (ADM) series generated by the "domino" model (Mazaud and Laj, 1989; Mori et al., 2013), we applied the criteria defined in Section 3 and included time intervals of "false" reversals or excursions into the chron lengths (see Fig. 7).

Perhaps the idea of a "domino model" of reversals (Mori et al., 2013) was properly incited by the theory of the liquid convection in the fast rotating planetary spherical shells. For a fluid shell heated from below (positive temperature gradient imposed between inner and outer boundary), convection starts in the form of columns outside the tangent cylinder parallel to the rotation axis (Fig. 1). The basic flow is a vortex motion around the axis of the column. The flow becomes quasi two-dimensional (geostrophic), minimizing any variation in Ω-direction (Proudman–Taylor theorem). Cyclonic and anticyclonic columns rotate in the same and in the opposite direction, respectively (Busse, 1975). In strongly driven dynamos the number of columns increases. Secondary flows are directed away from the equatorial plane in anti-cyclonic columns, but toward the equatorial plane in cyclonic columns. The helicity has therefore predominantly one sign in the northern hemisphere and the opposite sign in the southern hemisphere. The so-called α^2-dynamo mechanism can be thought of as a process where the helicity associated to each convective column produces its own magnetic field. The alignment with the rotation axis and the organized helicity guarantee that these individual contributions add up to form the dominant axial dipole field.

The numerical simulations show that enhanced CMB heat flux inside the tangent cylinder promotes dipole stability (Glatzmaier and Roberts, 1997; Glatzmaier et al., 1999), enhanced equatorial heat flux increases reversal frequency (Glatzmaier et al., 1999; Kutzner and Christensen, 2004; Olson et al., 2010), whereas reduced equatorial heat flux decreases reversal frequency and may even prevent reversals (Glatzmaier et al., 1999; Kutzner and Christensen, 2004). Simulations of the geodynamo suggest that transitions from periods of rapid polarity reversals to periods of prolonged stability (superchrons) may have been triggered by a decrease in CMB heat flow either globally or in equatorial regions (Biggin et al., 2012).

This aspect of the geodynamo simulations is in accordance with the result of a modified version of the "domino" model where a heat flux function is added; it shows that "the increase of the thermal flux along the axis of rotation leads to the partial suppression of the reversals of the field" (Hejda and Reshetnyak, 2012).

Aubert et al. (2008) identified flow upwellings as the cause of field reversals. These features rise from the inner-core boundary and produce inverse magnetic field. To some extent, the upwellings behave like tilted convective columns, at least what their role in the dynamo mechanism is concerned. Olson et al. (2014) derived a scaling relationship for the frequency of magnetic polarity reversals in numerical dynamos powered by thermo-chemical convection.

For the small, irregular, continued changes of the geomagnetic field (secular variations) and its abrupt changes – geomagnetic jerks (e.g. Duka et al., 2012), there is not yet a confirmed mechanism for their generation. Generally, it is almost accepted that such changes are generated by the fluid flow in CMB. The coupled dynamics of mantle and core convection must have had profound effects on the magnetic field in the more distant past (Heimpel and Evans, 2013).

The geomagnetic field models for the last 5 Ma (Johnson and Constable, 1997; Hatakeyama and Kono, 2002) based on paleomagnetic data show that the dipolar field presents the highest contribution to the total main field. As it can be seen in Fig. 2, the dipolar contribution to the secular time variation of the geomagnetic field is almost one order greater than non-dipolar one. The Fig. 2a shows the time variation of the dipolar moment calculated by the g_l^m ($l = 1$; $m = 0, 1$) Gauss coefficients of the gufm1 model (Jackson et al., 2000) as follows:

$$m = \frac{4\pi a^3}{\mu_0}\sqrt{\left(g_1^0\right)^2 + \left(g_1^1\right)^2 + \left(h_1^1\right)^2} \quad (1)$$

where a is the mean radius of the Earth (6371.2 km), and μ_0 the permeability of free space. The Fig. 2b shows the dipolar R_d and

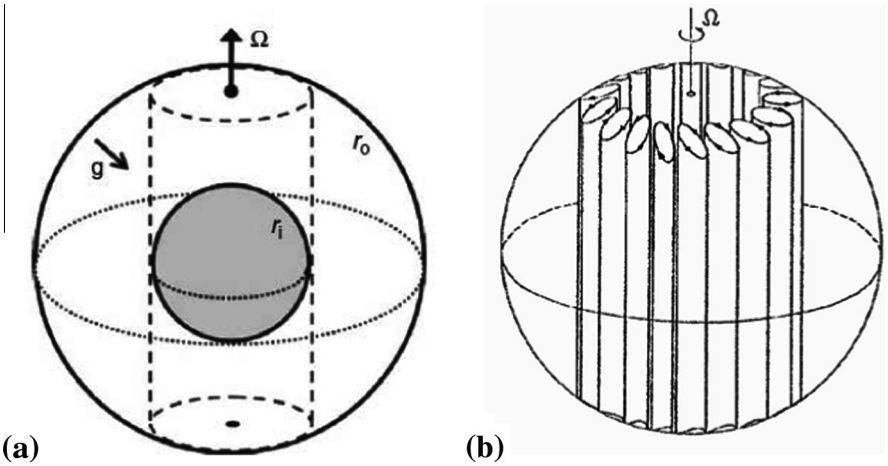

Fig. 1. Schematic pictures of: (a) fluid shell rotating with angular frequency Ω (dashed lines show the inner-outer core tangent cylinder), (b) distribution of the cyconic and anticyclonic columns outside the tangent cylinder.

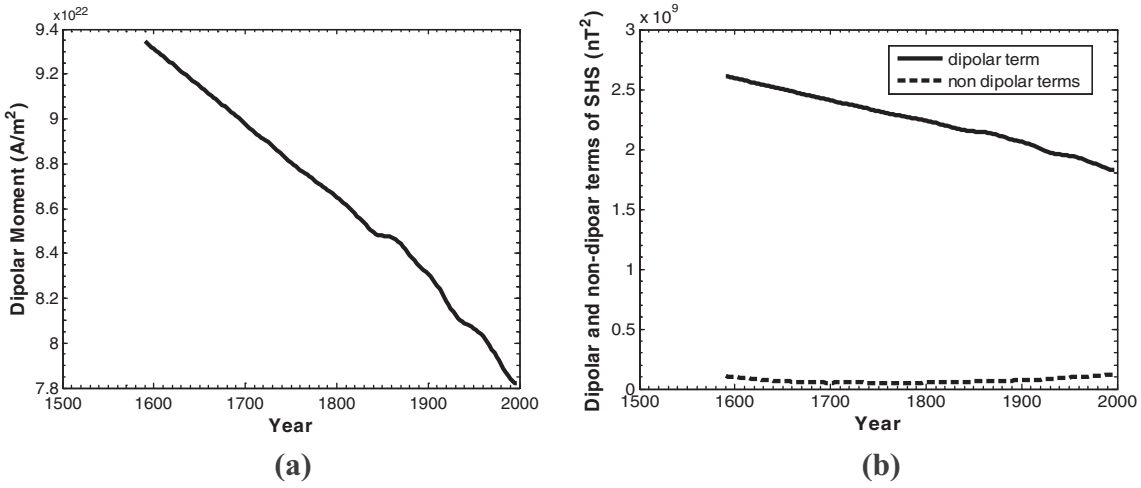

Fig. 2. (a) Time variation of the dipole moment and (b) spatial power spectrum of the dipolar and non-dipolar field according to the gufm1 model.

non-dipolar R_{nd} contributions to the spatial power spectrum calculated by the Gauss coefficients of the gufm1 model according to the respective formulas (Lowes, 1974):

$$R_d = \left(\frac{a}{r}\right)^6 \cdot 2 \cdot \left[(g_1^0)^2 + (g_1^1)^2 + (h_1^1)^2\right];$$
$$R_{nd} = \sum_{l=2}^{14} \left(\frac{a}{r}\right)^{2l+4} (l+1) \sum_{m=0}^{l} \left[(g_l^m)^2 + (h_l^m)^2\right] \quad (2)$$

at the Earth's surface ($r = a$). The gufm1 model (Jackson et al., 2000) was developed using historical and instrumental directional data (declination and inclination from navigational routes and ground observatories) from 1590 up to the present days. The intensity element was only constrained from 1832 to the present, because before that year there was not any instrument to measure it. For this reason, the authors assumed a linear behavior of the first Gauss coefficient g_1^0 before 1840 as shown in the Fig. 2a, evaluating τ_{SV} known as the secular-variation timescale (Lhuillier et al., 2011) to be on order of 500 yr for time rescale of the geodynamo simulations. Fig. 2b shows a linear decreasing of the dipolar term R_d during the last 400 years and an increasing trend for the non-dipole terms R_{nd}.

The short term changes (secular variation) and the long term changes (reversals) seem to have not the same statistical behavior. Whether the distribution of chron length obeys a Poisson (Cox, 1968) or Gamma law (Naidu, 1971) has been a controversial issue. Recent analyses of the geomagnetic polarity timescale (e.g. Lowrie and Kent, 2004) as well as numerical dynamo simulations (e.g. Wicht et al., 2009; Lhuillier et al., 2013) suggest that the distribution of chron lengths follows a Poissonian process (with no occurrence of superchrons); while distributions of reversal and failed reversal durations are better fitted by log-normal distributions. The secular variations can be considered as Gaussian process, although also the dipolar and non dipolar parts seem to have different statistical distributions (Constable and Parker, 1988).

Our simulated series of the dipolar geomagnetic moment showed a difference between statistics of long timescales and short timescales components (see Section 3). This will be compared with the statistical behavior of the long time series of the ADM according to the paleomagnetic database.

According to Mori et al. (2013), the "domino model" is appropriate to simulate reversals but it is not for secular variations. Differently from their position, we think that, choosing the values of "domino" model parameters in a proper way, e.g. by reducing the factors due to randomness, we can adapt the model to fit statistically the behavior of secular variations.

In this paper, after the description of the "domino model", we will confront our results of applying the model for "reversals"

simulation with Mori et al. (2013) results. Then we will show how the results depend on the model parameter values. Lastly, we will show that for an appropriate set of model parameters, we can apply the model to simulate secular variations that are in average close to SV given by different global geomagnetic field models of the recent past, such as CALS7k.2 (Korte and Constable, 2005), CALS10k.1b (Korte et al., 2011), and SHA.DIF.14k (Pavón-Carrasco et al., 2014).

2. The "domino" model

2.1. Standard "domino model" description

The term 'mechanism' of geomagnetic generation often refers to the process that generates axisymmetric poloidal field from axisymmetric toroidal field and viceversa. The mechanism is more easily elucidated in weakly driven dynamos (Davidson, 2013), where the flow outside the tangent cylinder is organized in well-defined geostrophic columns with negative helicity in the northern hemisphere and positive helicity in the southern hemisphere. Kageyama and Sato (1997) describe the mechanism of how the columnar convection cells convert an axisymmetric toroidal field, into the poloidal field of an axial dipole. This mechanism for poloidal field generation seems to operate in all published numerical dynamo models with columnar convection (Christensen and Whicht, 2007). The axisymmetric toroidal field can, in principle, be produced by an α-effect acting on the dipole field, or through shearing it by differential rotation in the mean zonal flow (Ω-effect). Depending on which mechanism dominates for the creation of the toroidal mean field, dynamos are classified as α^2 or α–Ω dynamos (Christensen and Wicht, 2007).

Recent numerical simulations of magnetohydrodynamics (MHD) for geomagnetism (Roberts and Glatzmaier, 2000; Kono and Roberts, 2002) seem to describe such dynamics. Inspired by these simulations, Mori et al. (2011) proposed a simple model ("domino" model) composed of many macro-spins which are each other interacting. This *coupled spin model* is based on the idea that the whole dynamo mechanism is described by global interactions of many small dynamo elements (macro-spins) (Nakamichi et al., 2011). This model naturally yields many of the observed features of the Earth's magnetic field: its time evolution, the power spectrum, the frequency distribution of stable polarity periods, etc. (Mori et al., 2011). In the case of the Earth, the dynamo element, that a macro-spin describes, is considered to be the Taylor cell in the iron fluid core produced and supported by the Coriolis force (Nakamichi et al., 2011).

Following Mori et al. (2013) description, the model consists of N macro-spins aligned along a ring and pair-wise interacting. The macro-spins are embedded in a uniformly rotating medium with unit velocity vector $\mathbf{\Omega} = (0; 1)$ along the rotational axis. Each spin $\mathbf{S}_i$ ($i = 1, \ldots, N$) has unit length and is described by its angle θ_i with respect to the rotational axis, such that $\mathbf{S}_i = (\sin\theta_i; \cos\theta_i)$. The orientation of the macro-spins can vary in time due to the forcing tendency of each spin to be parallel to the rotational axes and to the spin–spin interaction (coupling of spins) (Fig. 3). These two terms of interactions are expressed in the potential energy as the first and the second summation, respectively:

$$P(t) = \gamma \sum_{i=1}^{N} (\mathbf{\Omega} \cdot \mathbf{S}_i)^2 + \lambda \sum_{i=1}^{N} (\mathbf{S}_i \cdot \mathbf{S}_{i+1}) \tag{3}$$

where $\mathbf{S}_{i+1} = S_i$ when $i = N$. Here γ is a parameter characterizing the tendency of the macro-spins to be aligned with the rotation axis, while λ is a parameter characterizing the spin–spin interaction. Both these parameters should be negative as the respective terms are negative potential energy (attractive interaction). The scalar

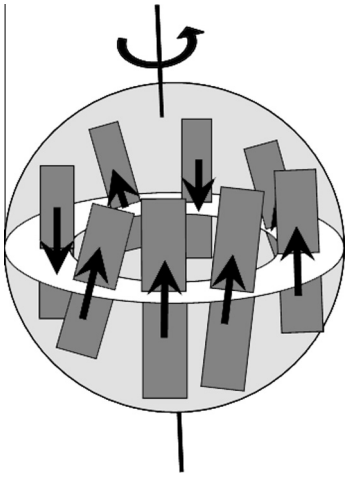

Fig. 3. Sketch of the standard "domino" model (according to Mori et al., 2013).

product squared in the first summation ensures that there is no preferred polarity. In the standard "domino" model or SCS (Short-range Coupled Spin) "domino" model (Nakamichi et al., 2011), the interaction is such that each macro-spin interacts with the two nearest neighboring macro-spins The macro-spin N interacts with macro-spins $N-1$ and 1, i.e. we are considering periodic boundary conditions.

The Lagrangian L of the system would be:

$$L = \frac{1}{2} \sum_{i=1}^{N} \dot{\theta}_i(t)^2 - \gamma \sum_{i=1}^{N} (\mathbf{\Omega} \cdot \mathbf{S}_i)^2 - \lambda \sum_{i=1}^{N} (\mathbf{S}_i \cdot \mathbf{S}_{i+1}) \tag{4}$$

A Langevin-type equation is set up as follows:

$$\frac{\partial}{\partial t}\left(\frac{\partial L}{\partial \dot{\theta}_i}\right) = \frac{\partial L}{\partial \theta_i} - \kappa \dot{\theta}_i + \frac{\varepsilon \chi_i}{\sqrt{\tau}} \tag{5}$$

where the term $-\kappa\dot{\theta}_i$ describes energy dissipation and the term $\frac{\varepsilon\chi_i}{\sqrt{\tau}}$ is a random force acting on each spin. The parameter κ represents the whole energy dissipation that, in MHD dynamos, includes the terms with viscosity parameters: ν, η, and term εT, with parameter ε representing the inhomogeneous heat generation from the inner iron core and the random perturbation from the other element spins (Nakamichi et al., 2011). Finally, χ_i is a Gaussian-distributed random number with zero mean and unit variance associated to each spin, which is updated each correlation time τ. Even the "minimal model" (Nakamichi et al., 2011), i.e. the model with no added dissipation and random terms in the Eq. (5), yielded almost the same features of the polarity reversals.

Substituting (4) into (5), the system of differential equations becomes:

$$\ddot{\theta}_i - 2\gamma \cos\theta_i \sin\theta_i + \lambda[\cos\theta_i(\sin\theta_{i-1} + \sin\theta_{i+1}) - \sin\theta_{i-1}(\cos\theta_{i-1} + \cos\theta_{i+1})] + \kappa\dot{\theta}_i - \frac{\varepsilon\chi_i}{\sqrt{\tau}} = 0 \tag{6}$$

where $i = 1, 2, \ldots N$; $\theta_0 = \theta_N$ and $\theta_{N+1} = \theta_1$.

After transforming the system of N equations of the second order (6) to a system of $2N$ equations of the first order, we integrated them forward in time with a 4th-order Runge–Kutta algorithm using an internal function of MatLab (ode45). The initial values of θ_i and time derivatives $\dot{\theta}_i$ are randomly distributed between 0 and 2π. The values of model parameters: N, γ, λ, κ, ε and τ are chosen in the intervals used by Mori et al. (2013) in their study of reversals. In the following section, some results that are different from Mori et al. (2013) results will be presented. The

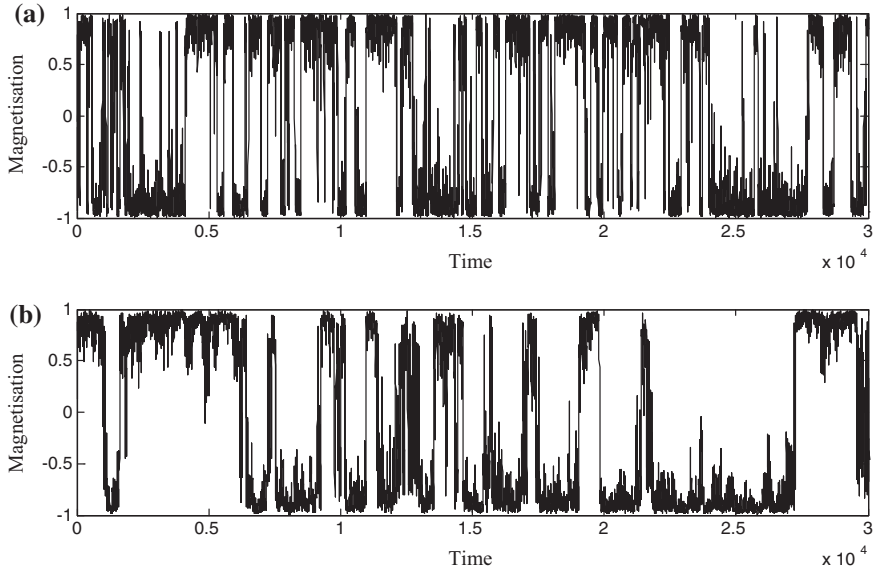

Fig. 4. Time series of magnetization generated by (a) standard "domino" model and (b) mean field "domino" model. Here are shown values for the first 30,000 time units.

output of each simulation is the cumulative orientation of all macro-spins, named magnetization:

$$M = \frac{1}{N}\sum_{i=1}^{N}(\mathbf{\Omega}\cdot\mathbf{S}_i) = \frac{1}{N}\sum_{i=1}^{N}\cos\theta_i(t) \tag{7}$$

that should correspond to the normalized axial dipolar momentum (ADM) of the geomagnetic field. It corresponds to the first Gauss coefficient g_1^0 of the multipolar expansion of the geomagnetic potential. The value of dipolar moment (DM) can be calculated as the output:

$$M(t) = \sqrt{\left[\frac{1}{N}\sum_{i=1}^{N}\cos\theta_i(t)\right]^2 + \left[\frac{1}{N}\sum_{i=1}^{N}sin\theta_i(t)\right]^2} \tag{8}$$

that corresponds to values of m given by (1).

2.2. "Domino model" with global interaction (mean-field domino-model)

Applying minor modifications to the standard version of the "domino model", such as the substitution of the Gaussian noise χ_i by a white noise, or the substitution of the interaction term $\gamma\sum_{i=1}^{N}(\mathbf{\Omega}\cdot\mathbf{S_i})^2$ by the term $\gamma\sum_{i=1}^{N}(\mathbf{\Omega}\cdot\mathbf{S_i})$, we received the same results as Mori et al. (2013): by the first modification the magnetization does not change much, except for slightly less frequent reversals, while by the second modification no reversals were observed.

The most important modification is the substitution of the local interaction of nearest neighbor macro-spins by a global interaction of each spin with all other spins. According to Nakamichi et al. (2011) this modification supplies two versions of "domino" model, the first ("standard") one named *Short range Coupled Spin* (SCS) and the second ("mean field") one named *Long range coupled spin* (LCS). The geodynamo considered two interactions among Taylor Cells that are produced respectively by non-linear flow (inward-winding or outward-winding) and by magnetic fields of the electric currents. The first one is a short-range interaction and the second one is a long-range interaction corresponding respectively SCS "domino" model of the macrospin interactions and LCS "domino" model of the macrospins interactions (Nakmichit et al., 2011).

Modifying the interaction term of the potential energy $P(t)$ (3), it becomes:

$$P(t) = \gamma\sum_{i=1}^{N}(\mathbf{\Omega}\cdot\mathbf{S}_i)^2 + \frac{\lambda}{2N}\sum_{i=1}^{N}\sum_{j>1}(\mathbf{S}_i\cdot\mathbf{S}_j), \tag{9}$$

and the equations derived from the modified Lagrangian become:

$$\ddot{\theta}_i - 2\gamma\cos\theta_i\sin\theta_i + \frac{\lambda}{2N}\sum_{j\neq i}^{N}(\cos\theta_i\sin\theta_j - \cos\theta_j\sin\theta_i) - \kappa\dot{\theta}_i + \frac{\varepsilon\chi_i}{\sqrt{\tau}} = 0,\ i = 1,\cdots,N. \tag{10}$$

In this case the numerical integration of the system of $2N$ ODE equations needed some modifications that considered multi-coupled equations and cyclic boundary conditions.

According to Mori et al. (2013), the mean-field model results in less frequent reversals, but shows otherwise qualitatively similar behavior. We compared the results of both versions of "domino" model for the same parameters values and confirmed the above conclusion. But in the quantitative aspect, the comparison of statistical behavior (e.g. in terms of power spectrum density – PSD) between magnetization series generated by both versions of "domino" models and polarity reversals series supplied by paleomagnetic data, there is better accordance for the "mean field" version. In the Fig. 4 we show the time series of magnetization for the first 30,000 time units (Fig. 4a for standard model and Fig. 4b for the mean field model) and the respective statistical analyses in Fig. 5 (Fig. 5a for standard model and Fig. 5b for mean field model). The time series of polarity reversals during 157.53 Myr provided by Cande and Kent (1995) with additional short subchrons summarized by Lowrie and Kent (2004) is shown in the Fig. 6a and the respective PSD is shown in Fig. 6b. According to the values of line slopes (power indexes – m), one can see that statistical behavior for "mean field" model (Fig. 5b) is better matched to the statistical behavior of long series of polarity reversals of geomagnetic field (Fig. 6b). Therefore we applied this model version to simulate series of dipolar magnetic moment that are comparable with that given by the geomagnetic field models like CALS7K.2, CALS10k.1b, and SHA.DIF.14k.

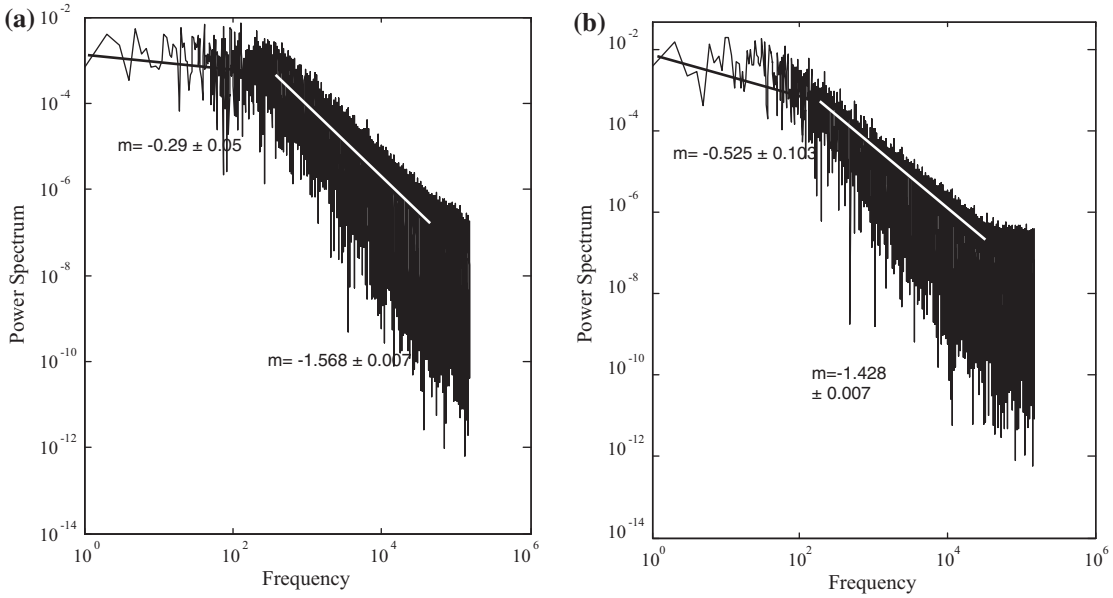

Fig. 5. Power spectra (PSD) of the magnetization series of 300,000 time units generated by (a) standard "domino" model and (b) mean field "domino" model with the same values of model parameters. The values of the slopes for each part of the spectrum are shown in the graphs.

3. Some results of "domino" model

We present here some numerical results of the "domino" model. Please note that there are some little differences or even discrepancies with Mori et al. (2013) results that we will try to explain. The output of simulations i.e. the time variation of magnetic moment *M*, is similar as can be seen by comparing the Fig. 2 of Mori et al. (2013) with our Fig. 4a. These graphs are for the same values of model parameters: $\gamma = -1$, $\lambda = -2$, $\kappa = 0.1$, $\varepsilon = 0.4$, $N = 8$, the same number (30,000,000) of steps of running the Runge–Kutta subroutine (output results every 100 steps) and with the same value of $\tau = \Delta t = 0.01$ as the Runge–Kutta integration step of each run of subroutine. τ is also the correlation time, i.e. the time of updating the random number value (χ_i). The initial conditions were taken: θ_i - random uniformly distributed between 0 and 2π, while $\dot{\theta}_i = 0$ at $t = 0$. Our resulting series, even when we applied the same error tolerance (10^{-10} absolute tolerance for each component as their absolute error bounds equal to 10^{-10} for θ_i), contains more frequent passes from positive to negative values i.e. zero-crossing values, than their series. But the greatest difference between our series of magnetization and their respective series is related to the power spectrum density of these series. Comparing Fig 3 of Mori et al. (2013), and our Fig. 5a, one can see the difference of the statistical analysis of the whole time series. Their power spectrum over a large range comprising most of the reversals, follows a power law with an exponent of about -1.7, is flatter (power law with the exponent of 0.15) for small frequencies or long polarity chrons and is a steeper decrease at high frequencies (power law with the exponent of -6.1). Differently, the power spectrum for our respective series of magnetization (Fig. 5a) follows two different power laws: the first one for the low frequencies (long timescale components) with the exponent -0.29 and the second one for the high frequencies (short timescale components) with the exponent -1.57. In fact, most of power spectrum analyses of paleomagnetic VADM series shows, similarly to our analyses, only two different slopes in the log–log plots [see Aubert et al. (2010), where one can find the analyses for Sint-2000 (*red*, Valet et al., 2005) and PISO-1500 (*blue*, Channell et al., 2009)].

We think that the important differences between our results and Mori et al. (2013) results can be explained by the two following reasons. The first reason is that although both groups (Mori et al., 2013 and us) used essentially the same Runge–Kutta method of integration for the numerical integration of the equation system (6), they implemented it in different software platforms. More precisely, Mori et al. (2013) implemented a traditional Fortran subroutine named RK4 (Press et al., 1996). According to their paper, they used "two different algorithms from the ODEPACK, a predictor–corrector scheme after Adams (suitable for non-stiff systems) and a backward differentiation scheme after Gear (for stiff cases)" and both gave the same results as the Runge–Kutta scheme (RK4), once the error tolerances were chosen small enough. Even when they reduced the time step of the Runge–Kutta routine, the overall statistical behavior did not change.

Instead, we used ode45 function of the MatLab platform. This function is based on "Dormand and Prince" method of Runge–Kutta algorithm (Dormand and Prince, 1980). In this method, the error terms in the higher order approximation are minimized and in some sense overcome the problem of under estimating the local error. We believe that ode45 of MatLab is effectively a higher order method than RK4. It produces error oscillatory that grows in between the integration points due to the interpolation, but the error at the true steps grows more slowly than the error for RK4. We can affirm that ode45 is more precise but slower than RK4 (for example, one simulation with 30,000,000 steps of integrations by ode45 lasted about two days clock time in a PC: Pentium® dual-core CPU E5500 @ 2.80 GHz, 2.79 GHz, 1.96 GB RAM). We also changed the order of absolute error tolerance from 10^{-6} to 10^{-10} (extending the clock time from two days to one week) and did not notice any significant differences in the overall statistics of the output magnetizations series. In order to verify quantitatively the differences between the different methods of integration (fortran RK4 and ode45), the execution of the respective Fortran code used by Mori et al. (2013) is needed. We tried to do this with a testing code[1] that was not running providing several compilation errors. After fixing the code, we received unexpected results, in particular no reversals occurred even after 300,000,000 conventional temporal steps. Further check, correction and rewriting the Fortran code of the

[1] The testing code was send us from a collaborator of one (SD) of the authors of Mori et al. (2013).

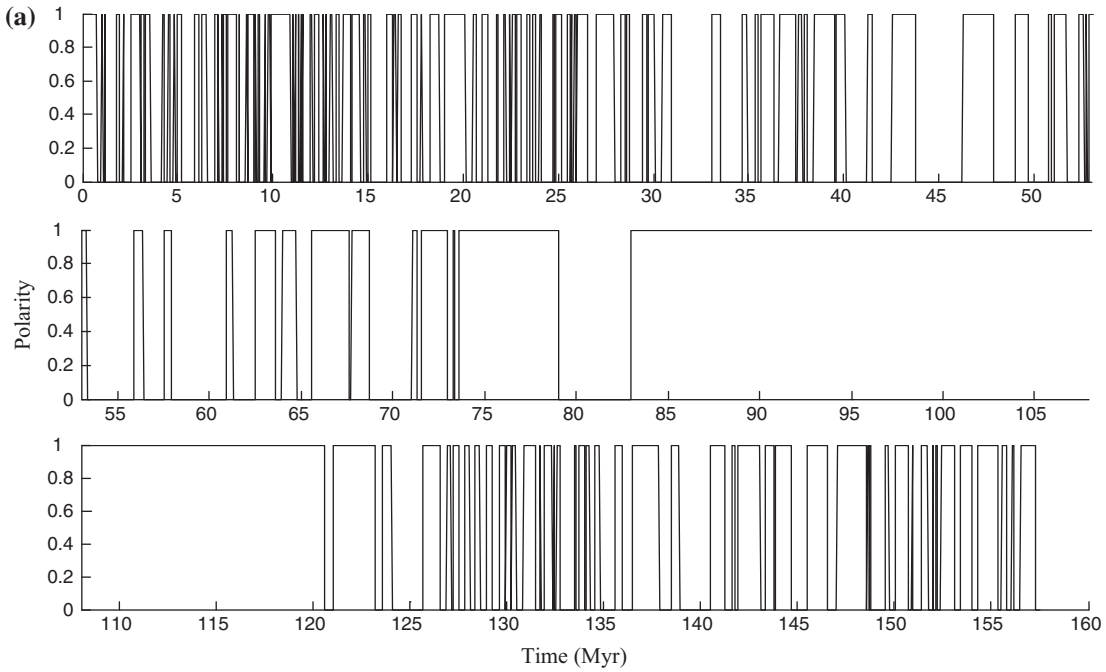

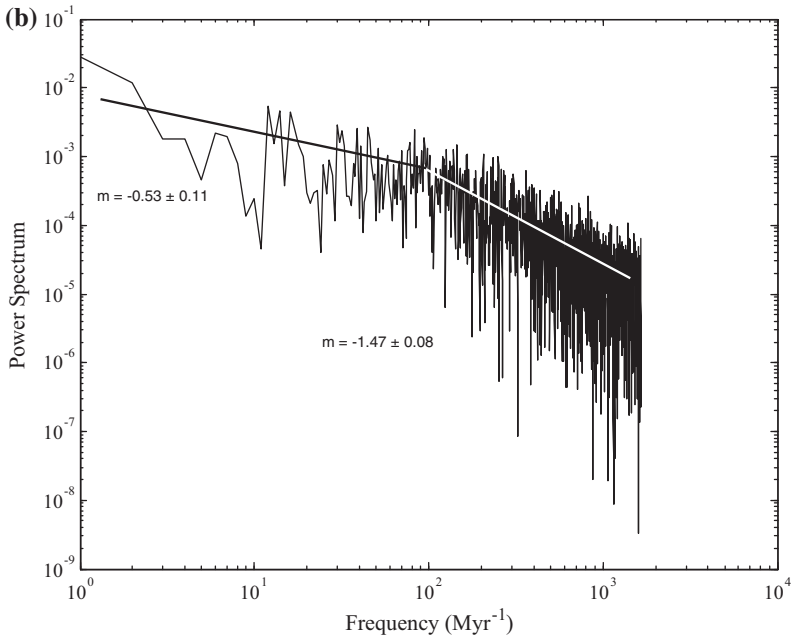

Fig. 6. (a) The time series of the polarity reversals for the period of 157.53 Myr provided by Cande and Kent (1995) and (b) its power spectrum (PSD).

whole procedure would need an extra huge work that is beyond the aims of this study.

The second reason that could explain the differences is that, the two groups used different functions to generate Gaussian distributed random numbers. Mori et al. (2013) used the Fortran subroutines RAN1 and RAN3 (Press et al., 1996), while we used the internal function random ('normal', 0, 1) of the MatLab platform. Both methods supply a Gaussian distribution, expected to have zero mean ($\mu = 0$) and unit standard deviation ($\sigma = 1$). To assess the overall difference between the two functions, we have generated random numbers by means of both ways (Fortran and MatLab), and we have seen very slight differences from the expected values. However, we noticed that the MatLab results are a little better than the Fortran results. In average, after several generations of the long series (100,000 values) of random numbers, we found: $\mu = 0.003341$ (Fortan); $\mu = 0.00171$ (Matlab); $\sigma = 0.998048$ (Fortan) and $\sigma = 0.999084$ (MatLab).

Not all zero-crossings of magnetization are considered as reversals by Mori et al. (2013). They considered "true reversals" only those passes that cross the central band of $M = [-0{:}5;\ 0{:}5]$. Indeed, we applied another criterion for identifying the "true reversals". We considered duration of a reversal the time interval during which the magnetization goes from the band 0.5 ± 0.1 to the band -0.5 ± 0.1 or vice versa with a change greater than 0.9. According to this criterion the mean time interval between the successive zero-crossings resulted 17 time units, i.e. the mean

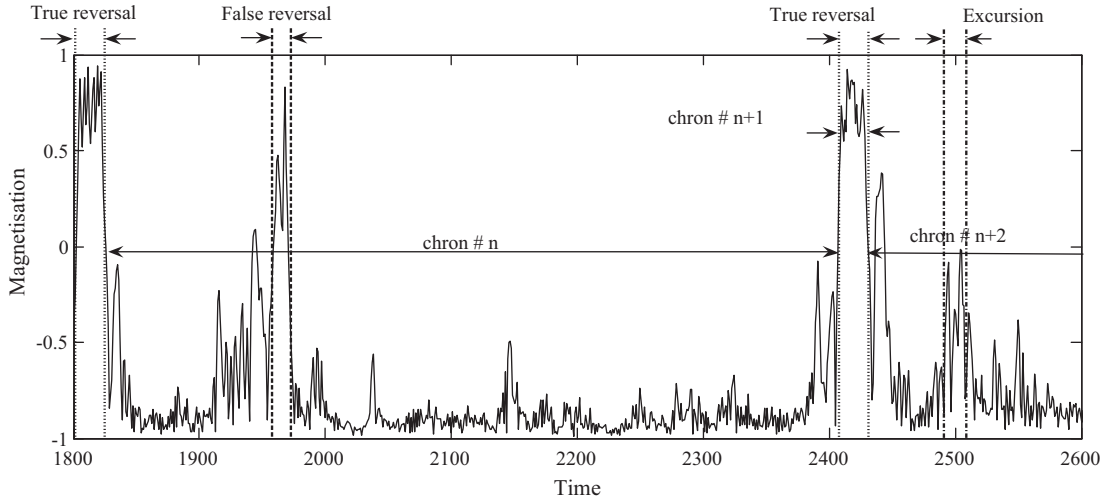

Fig. 7. A short sequence of the time series of magnetization generated by standard domino model, where our criterion of defining the "true" (between dotted lines) and "false" (between dashed lines) reversals is illustrated. "False" reversals and excursions are included in the chron duration.

duration of reversals is 17 time units. Then we have considered as true reversals those that last at least 17 output units, i.e. when the time interval between the successive crossing zeros is equal or greater than 17 units. According to our calculations (see below for the time scale of our model), these 17 time units correspond to about 20,500 years of real time, which is near the minimum time of a real complete inversion of the geomagnetic field (Gubbins, 1999). So our criterion considers the chrons longer than 17 time units, including in chrons not only "false" reversals (when the next zero-crossing is near than 17 time unit) but even "excursions" (see Fig. 7). We made this choice because we think it is normal to consider true reversals of the geomagnetic field as those that produce stable polarization, i.e. enough longstanding chrons. Our choice is further supported by noticing that, in our time series of magnetization, almost all zero-crossings of magnetization below 17 time units ("short-living" inversions) are fluctuations with very small amplitudes.

We also checked if the discrepancy between Mori et al. (2013) results and ours is due to the difference between our criteria and their criteria of decision about the true reversals. Applying their criteria to our series, we found almost the same discrepancies. Therefore, we think the reason is due to the differences in the used random generated functions and the algorithms for the integration.

Regarding the correspondence between the running step of the subroutine and time interval of the model, the reasoning is based on observing the mean number of reversals in the time series generated by several runs of the same parameters simulation. In our example there are 1339 reversals (averaging several runs). The mean time *mtr* between two consecutive reversals, i.e. the average length of chrons, is calculated as the ratio of the length of the time series with the number of reversals identified in this series. So, for our simulation of the standard "domino model", $mtr = 224$ time units. According to the polarity reversal series of paleomagnetic data (Fig. 6a), considering only chrons with duration shorter than 1 Myr, we find that the mean of chron durations is about 269 kyr, therefore we approximated the *mtr* for the geomagnetic field to 270 kyr. The difference of our result from Mori et al. (2013) result (300 kyr) is probably due to the difference of full series length (ours is 157.53 Myr, theirs is 166 Myr). Equaling the 224 units of time of the model to the 270,000 years of the real geomagnetic field, results that one unit of time of the model is the equivalent of about 1200 real years. So the full run spans a period of nearly 360 Myr. We have considered this time scale valid for all time series generated by the standard "domino" model.

Regarding the magnetization and chron length (time between reversals) distribution, one can compare our Figs. 8a and 9a with the respective figures of Mori et al. (2013), (their Figs. 3b and 4b). The distribution of the magnetisation peaks near ±1 with a wide and deep valley between them (this is the same in their Fig. 3b and our Fig. 8a). This reflects the fact that the reversal times are short events compared to the average duration time between them and that the spins are most of the time closely aligned with the rotation axis. In addition, the horizontal component of dipolar moment calculated as the output:

$$M_h = \frac{1}{N}\sum_{i=1}^{N} \sin\theta_i(t) \tag{11}$$

is most of the time close to zero (see Fig. 8b).

In order to get the distribution of the chron duration (less than 1 Myr) in the paleomagnetic polarity reversal series (Fig. 6a), we have used the so named "Lomb" method for unevenly sampled data (Press and Rybicki, 1989). The result is shown in the Fig 9b. As it can be seen, both distributions (exponential and lognormal) well fit the data. Therefore we cannot select if the distribution is a Poissonian (exponential) or a lognormal (e.g. Ryan and Sarson, 2007). Fig. 9a shows the chron duration distribution of the magnetization series (Fig. 4a) generated by the standard "domino" model, where only chrons that last less than 830 time units (equivalent to 1 Myr) are considered. As it can be seen this distribution, as in the case of the paleomagnetic data, is well fitted by a lognormal distribution or an exponential distribution.

Further we analyzed the mechanism which lies underneath the domino model by studying the time variation of magnetization for each macro-spin in case. As indicated by Mori et al. (2013), we noticed that when a large fluctuation of a macro-spin is successively transferred to neighbor macro-spins than a true reversal happens. Otherwise, aborted reversals (quick return to the previous orientation of magnetization) or excursions (reducing the value of magnetisation but not inversion) could happen.

4. Dependence on parameters

The dynamo model we are investigating has six independent parameters: N is the number of macro-spins which represents the number of magnetic dipoles, γ models the tendency of the macro-spins to be aligned with the rotation axis, λ models the magnetic interaction between macro-spins, κ models the friction

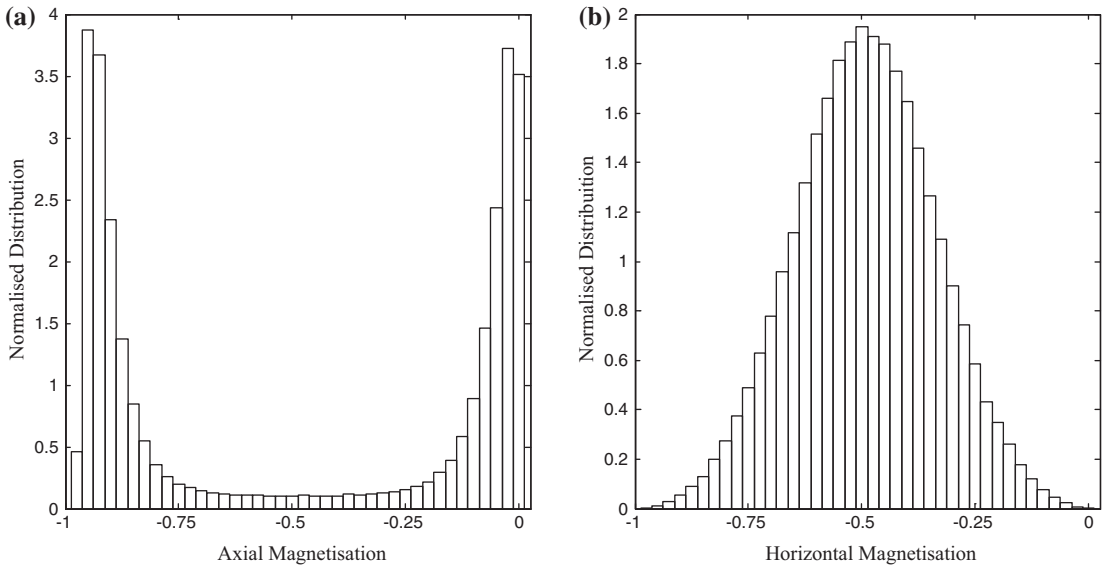

Fig. 8. Magnetisation distribution for (a) axial magnetization, (b) horizontal magnetization.

(dissipation), ε models the random forces, and τ represents the interval of time after which the random χ_i number is updated. Varying the parameters values in the same intervals like as Mori et al. (2013), we obtained similar results about the dependence of *mtr* against the parameters. The obtained graphs of these dependences are similar to the Fig. 8(a)–(d) of Mori et al. (2013), therefore are not shown here. The physical meaning is the same: a decreasing of γ and λ (while their absolute magnitude increases because these parameters take negative values) means an increasing tendency of macro-spins to align with the rotation axis and a stronger interaction between them, leading to less numerous reversals, so the *mtr* value will be greater. An increasing κ (which is positive) means that the friction, which prevents the spin reversal, is greater and the reversals are fewer, so the *mtr* value increases. An increasing of ε means that the intensity of the random forces is greater, so the random character of the model is amplified and the reversals are more numerous and *mtr* decreases. We conclude that the parameter which affects mostly the results is κ as found in Mori et al. (2013).

We also analyzed the change of *mtr* versus the increase of τ and Δt. An increase of Δt (0.01, 0.05, 0.1) did not show qualitative or quantitative changes in the outcome results. When we changed τ and Δt ($\Delta t = \tau$), a linear dependence was observed. So such linear dependence is solely the contribution of the τ change. As it is seen from equations (6), increasing τ is similar to decreasing ε, but because these equations are scaled linearly with ε and linearly with $\tau^{-1/2}$, the increase of *mtr* is smaller in the case of increasing τ.

An unexpected result was the dependence of *mtr* against the dipole number. We obtained different dependence (Fig. 10a and b). It is clear that between 1 macro-spin (no interaction with other macro-spins) and two macro-spins where there is one λ-term more, *mtr* should increase. As the number of macro-spins increases further, the number of the equations of the system (6) increases. The increase of the number of the interaction terms (which tend to keep macro-spins aligned with each other) produces the increase of the *mtr*, while the increase of number of the random terms (which tend to destabilize the system of macro-spins) produces a decrease of *mtr*. As it clear from Fig. 10, from $N = 2$ to $N = 10$, which correspond to the maximum *mtr* of our results, the effect of the increase of the interaction terms overpasses the destabilizing effect of random terms and the *mtr* value increases. Nearly the same is observed by Mori et al. (2013). After $N = 10$, it seems that the destabilizing effect of the random term

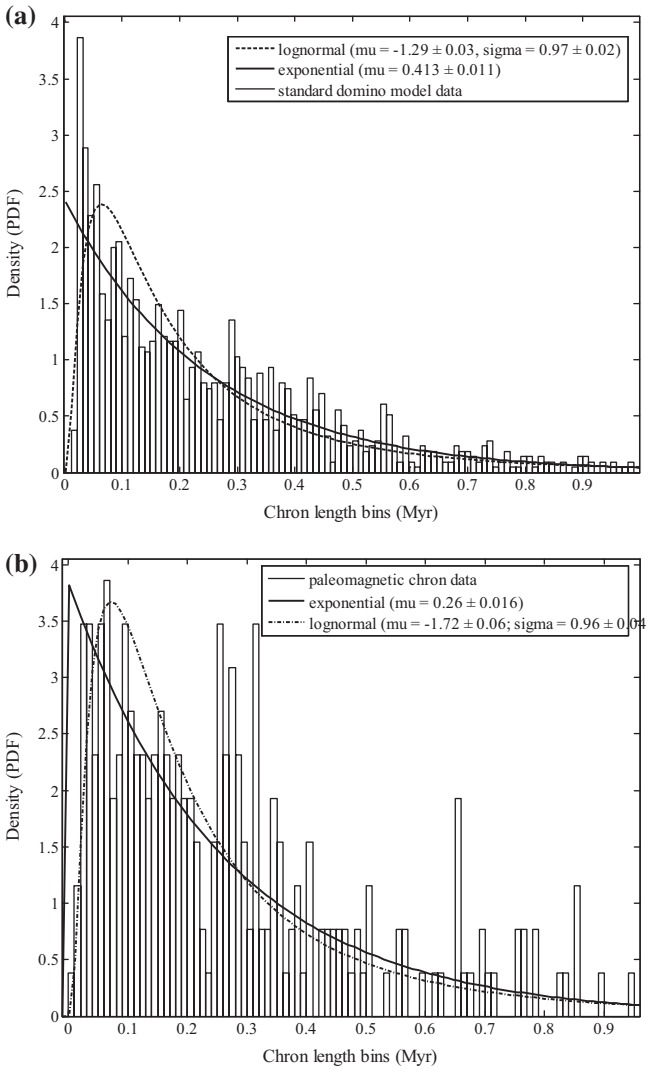

Fig. 9. Chron length distribution (lengths are less than 1 Myr) for (a) a magnetization series generated by the standard "domino" model and (b) the series of polarity reversals (both series with the same length of 157.25 Myr) and their fitting to the different kind of known distributions (exponential, lognormal).

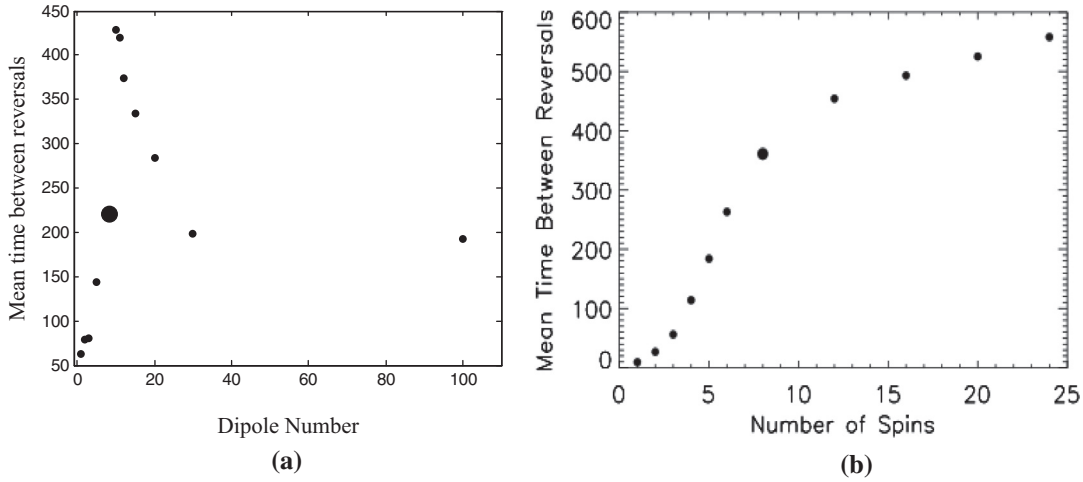

Fig. 10. The dependence of *mtr* against the dipole (macro-spins) number: (a) our results, (b) (Mori et al., 2013) results. The largest circle denotes the number $N = 8$, that is usually used in the standard "domino" model simulations.

increase compensates the effect of interaction term increase and *mtr* seems to be almost constant. But our graph (Fig. 10a), in contrast with the results in Fig. 10b (Mori et al., 2013), shows a decreasing after $N = 10$. We explain this decreasing by the predominance of the effect of the increase of the random terms in comparison to the effect of the increase of the number of interaction terms. Then, after $N = 30$, the further increase of both effects becomes negligible, the model saturates and *mtr* remains constant. The saturation is observed even in the graph (Fig. 10b) represented by Mori et al. (2013), but the falling part of our graph is not found in their respective graph. The *mtr* continues to increase, even slightly, without reflecting the effect of the increase of random terms. In our opinion, the reason of such divergence is the difference between our series and their series of magnetization, even then these series are generated by the same set of parameters.

5. Applying Mean-field domino model to model the SV of dipole moment

According to the classical electrodynamics, the magnetic field produced by each single macro-spin of the "domino model" should affect all the others. Therefore, we considered the macro-spins as immersed in magnetic "mean-field" formed by the superposition of their own magnetic field. This model named as LCS is described by Nakamichi et al. (2011), where the relation of this model to geodynamo is explained.

The number of reversals in the magnetization series generated by this model is smaller than the number of reversals in the respective series generated by the standard model with the same set of parameter values. This is expected because the interaction between all macro-spins implies that there are more interaction terms than in the standard model, so the system is more stabilized. In a full run (in Fig. 4b, only 30,000 first units are shown), there were observed in average 200 true reversals and *mtr* = 1,500 units of time. Following the same reasoning as in the standard model, considering the *mtr* length equal to 270,000 years of real time, the full run corresponds to 54 Myr. We will use then this time scale, which is different from the time scale of the standard domino model, in all next simulations of the time series generation for the SV modeling.

Although the short term changes (secular variation) and the long timescales changes (reversals) seem to have not the same statistical behavior, it is now widely thought that excursions and

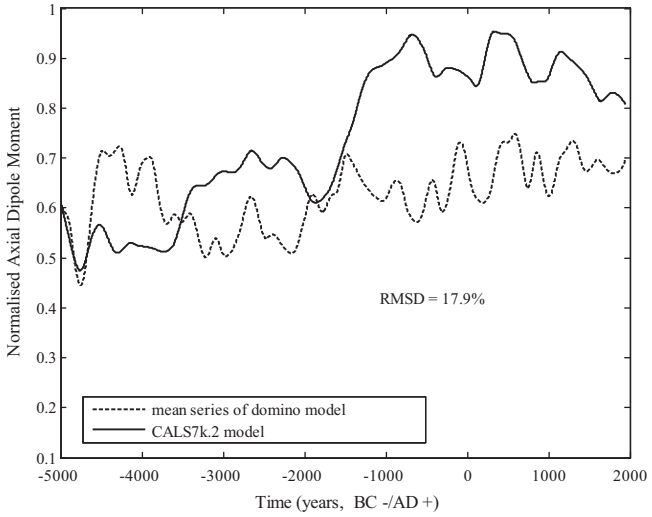

Fig. 11. Time series of the SV of the ADM supplied by CALS7K.2 model and the respective averaged time series generated by the mean field "domino" model.

reversals are natural outgrowths of SV (Gubbins, 1999; Biggin et al., 2008; Lhuiller and Gilder, 2013).

According to Mori et al. (2013), their domino model "provides a convincing statistical representation of the geomagnetic field reversals process". As they thought that the spins represent convective columns of the dynamo process: "A stable polarity can only established when the majority of these entities cooperate and produce field of the same polarity. Random forcing counteracts this and may sometimes be violent enough to cause a spin to flip significantly and leave the team. This may cause its neighbors to follow and ultimately lead to a reversal. The magnetic upwellings identified in full 3D dynamo simulations by Aubert et al. (2008) could be these events". Regarding secular variations, they conclude that: "Secular variation, which is mainly determined by the details of the convective flow dynamics, is certainly not captured correctly" by their "domino" model. Therefore, the authors conclude that the domino model does not reproduce correctly the SV of the geomagnetic field. In fact the SV occur on a wide band of time scales. The rapid SV changes and the slow ones are probably controlled by different processes. It is true that we cannot produce correctly all changes of SV by running the "domino" model, but we

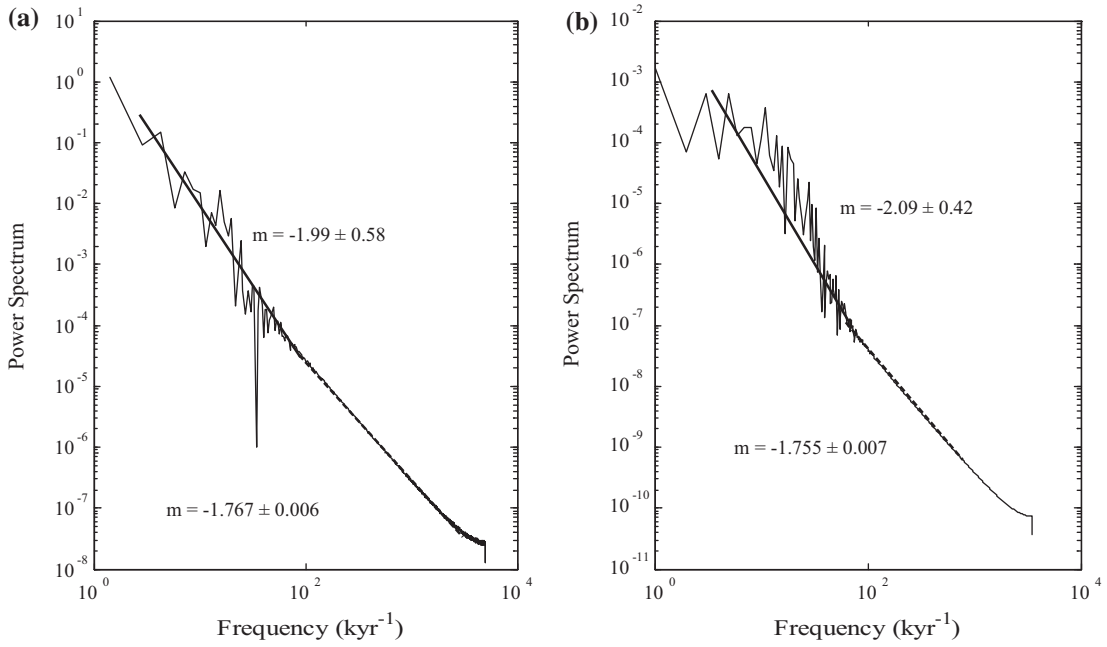

Fig. 12. Power spectrum (PSD) for: (a) the time series of ADM provided by CALS7K.2 model and (b) the respective time series generated by the mean field "domino"model.

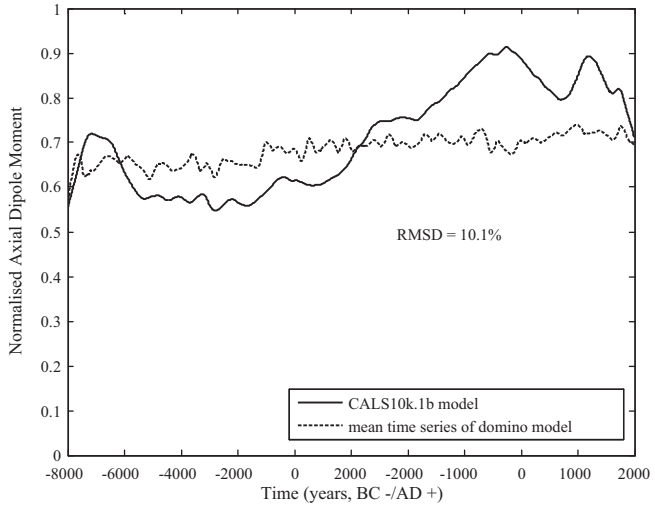

Fig. 13. Time series of the SV of the ADM supplied by Calsk10.2b model and the respective averaged time series generated by the mean field "domino" model.

can use "domino" model to generate long series of SV that have a very similar statistical behavior as the long series of observed SV, at least for the dipolar field. We think that Mori et al. (2013) conclusion was correct only for the range of the set of parameter values of the model chosen by them. If we consider the reversals as part of the SV, why do not we try to find a more appropriate set of the model parameters to fit SV on a wide timescale? We tried to do this, by reducing, in particular, the value of the ε parameter which affects the random terms of the system equations.

The time series of the magnetic moment generated by such new model were then compared with time series of the dipolar moment deduced by the models based on paleomagnetic, archeomagnetic and historical data of the geomagnetic field in different places of Earth.

The chosen paleomagnetic field models for our analysis are the CALS7k.2, CALS10k.1b and the SHA.DIF.14k which provide the secular variation of the dipolar and non-dipolar geomagnetic field during the last 7, 10, and 14 millennia, respectively. The first two models (CALS7k.2/10k.1b) were built using all the available paleomagnetic data for the last millennia, i.e. archeomagnetic data, lava flow, and lake sediment data. The last model (SHA.DIF.14k) was developed using only archeomagnetic and lava flow data, because it was thought that the sedimentary paleomagnetic data would have deteriorated the quality of the final model (Pavón-Carrasco et al., 2014). The effect of not including sediment data in the SHA.DIF.14k model can be clearly seen in the model predictions showing geomagnetic field elements with higher temporal variability than the CALS models, the latter due to the smoothed sediment data. All these paleomagnetic models present a lower resolution (spatial and temporal) than the previous cited gufm1 model or other instrumental models, as the IGRF-11 (Finlay et al., 2010), because the paleomagnetic data can provide a robust information only up to the degree 3/4 of the spherical harmonic terms of the geomagnetic field (Korte et al., 2011; Pavón-Carrasco et al., 2014, among others). This limited resolution is due to the own paleomagnetic data which present high dispersions and uncertainties, and, in addition, their spatial and temporal distribution is sparse, characterized in particular by a scarce number of data in the South Hemisphere and by most of them in the Eurasian continent (see Fig. 1 in Pavón-Carrasco et al., 2014). However, in spite of such limitations, the models can be considered a good representation of the temporal behavior of the dipolar moment magnitude, given only by the first spherical harmonic contribution (degree 1).

In order to generate the respective time series of dipolar magnetic moment by "domino" model, we have chosen those sets of model values, which produced the longest *mtr* (the smallest number of reversals). We made this choice because the simulated series should last some thousands years of the real time and there should not occur any polarity reversal (presently no polarity reversal has not occurred yet). From the simulations performed by us, we found that the mean-field domino model with 10 macro-spins has the greatest *mtr* value. However we take the value $\tau = 0.01$, as in the standard model, because the contribution of its increment is less than the one given by the other parameters.

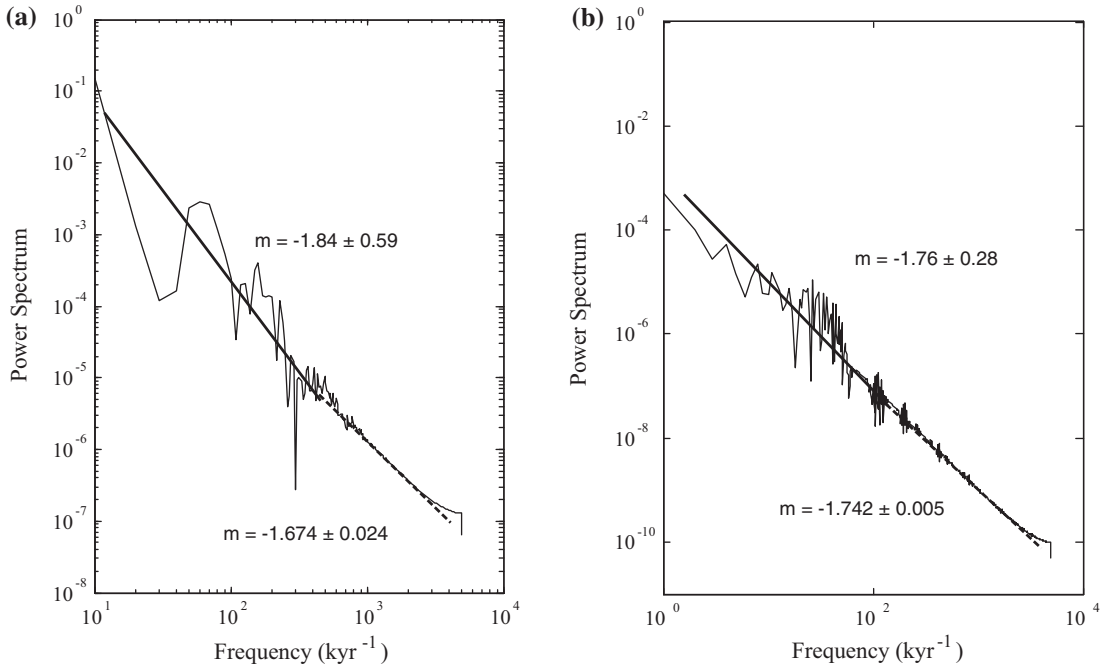

Fig. 14. Power spectrum (PSD) for: (a) the time series of ADM supplied by Calsk10.b model and (b) the respective time series generated by the mean field "domino" model.

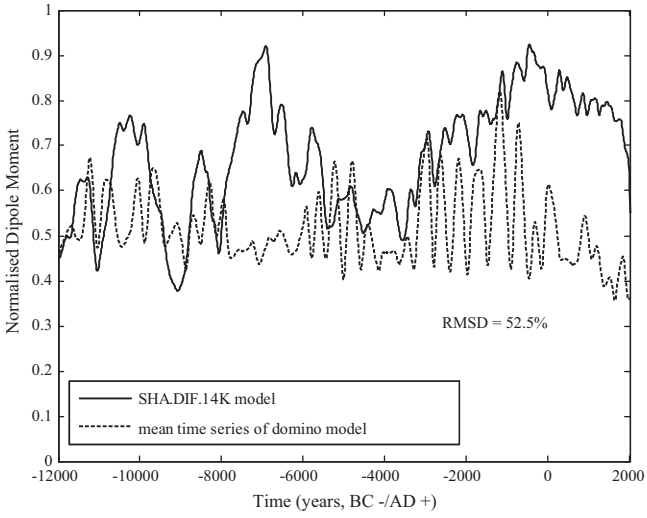

Fig. 15. Time series of the SV of the DM supplied by SHA.DIF.14 model and the respective averaged time series generated by the mean field "domino" model.

When we previously simulated the domino model for long periods of time (to get the reversals), we took the initial angles θ_i as randomly uniform-distributed while the initial angular velocities were considered to be 0 (the macro-spins were considered to be initially at rest). The former set of initial conditions determines the magnitude of the dipolar moment (Eq. (7)) at $t = 0$, while the latter set determines the initial velocity of change of the magnitude of the dipolar moment (difference of second and first value of the magnetic dipolar moment over the interval of time passed between these two estimated values). The full runs have no other models to be compared with, so we have free hand in the choice of initial conditions. In the cases of SV time series simulations, which will be averaged on different runs and will be compared with real time series (SV) of the above mentioned models, the initial value of the magnetic dipolar moment and a non-zero initial velocity of change of its magnitude must be given the same for the different runs of the simulation. Our algorithm of integrations of the Eq. (10) starts when these initial conditions are fulfilled. Since in the cases of CALSK10.b and SHA.DIF.14k models, series show a very small initial velocity of dipolar magnetic change, at least three or four orders smaller than the values of the magnetic dipolar moment itself, we considered the initial velocity as zero in our simulations. In these cases, in order to cancel short and small fluctuations of the values in the time series of magnetization obtained by the all runs of simulations, the generated time series are de-noised by using the MatLab wavelet packet (Duka et al., 2012). The generated time series have all undergone the same level of de-noising.

We performed several simulations in order to identify the set of values of the independent parameters for the "domino" model which better follow the SV models. It resulted that, among many obtained simulations, the best agreement between synthetic and model SV series was achieved by the set of parameters values: $\gamma = -2.1$, $\lambda = -2.0$, $\kappa = 0.015$, $\varepsilon = 0.2$, $\tau = 0.01$, $N = 10$.

The initial dipolar moment in the series generated by "domino" model, is imposed to be approximately the same as the normalized initial value of the respective series of SV models (normalized means that all values of the ADM or DM series are divided by a maximum value of 10^{23} A/m^2). The simulations showed that even for the same set of parameters values, the random terms affect the results in such a way that practically we cannot obtain exactly the same time series of magnetization twice. Even if we fully de-noise the time series, we should take in mind that this series is obtained by solving the system equations part of which is composed by the random terms. In order to reduce such effect, we have averaged time series generated by 30 different runs, but with the same parameters and initial conditions. Every element of the averaged time series is the mean of the respective elements from the generated 30 series. Then we calculated a deviance vector as the difference between the SV model time series and the mean series generated by domino model. Next we calculated the 2-norm of this

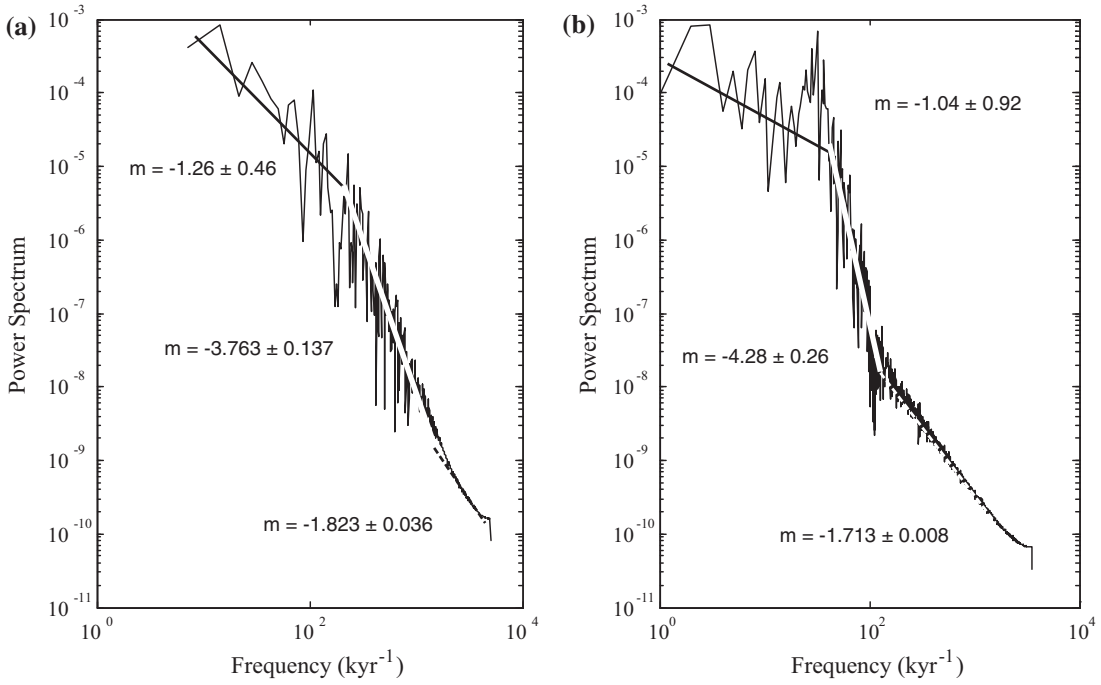

Fig. 16. Power spectrum (PSD) for: (a) the mean time series generated by the mean field "domino" model and (b) the time series of DM supplied by Sha.dif.14 model.

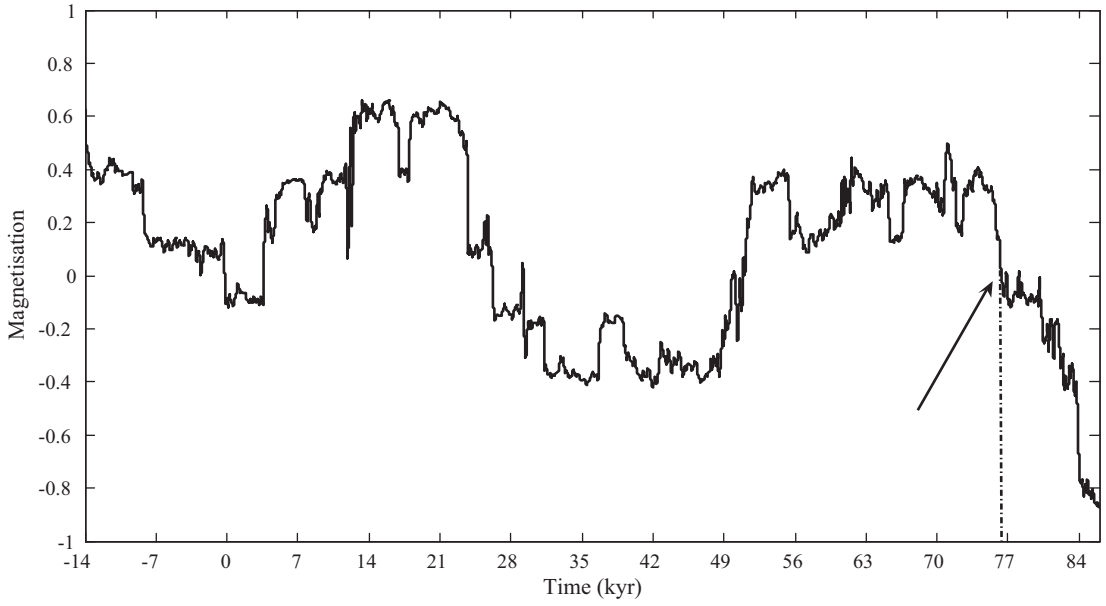

Fig. 17. The mean of different 100,000 yr long time series generated by different runs of the "domino" model. A "true" reversal is detected at about 75,000 yr of the future time.

deviance vector, a calculation that yields the RMSD (Root Mean Square Deviation).

We begin our comparisons with the CALS7k.2 model which gives the SV series of ADM (Axial Dipolar Moment) for the last 7 kyr. In this case, we have imposed initial condition not only on the initial value of the dipolar moment but also on the sign of its time derivative (it should be negative). Imposing such condition increased the clock time of execution about 10 times more than the normal time of one run. Therefore, we limited the number of runs to 15, and the averaged series (without de-noising) is shown in Fig. 11. Comparing this series to the CALS7k.2 series (Fig. 11), one can see the differences (RMSD = 17.9%). There is a good match of both curves at the beginning then there are increasing and decreasing of the differences between curves. As it can be seen in the Fig. 12, the statistical behavior of magnetization series generated by the domino model is very close to that of CALS7K.2 model, not only qualitatively (the power spectrum shape), but also quantitatively (the slopes *m* for both PSDs are shown in the figure).

The second model we take in consideration is the CALS10k.1b which provides the SV series of ADM of the geomagnetic field for the last 10 ka. It represents an extension of the previous model with new and older paleomagnetic data, where it is applied a

bootstrap algorithm to obtain the final set of Gauss coefficients (Korte et al., 2011). In this case, we followed the procedure of de-noising and averaging the 30 series of magnetization generated by 30 runs of the "domino" simulations with the same parameter values and initial condition values (zero initial velocities). As it can be seen (Fig. 13), the match of both curves (averaged series generated by "domino" model and normalized series of ADM of CASL10k.1b model), is better than in the first case (RMSD = 10.1%). While Fig. 14a and b, show the PSDs of the respective series of both models. Both PSDs have two-slope shapes (in the log–log plots) where the slope coefficients (m) are still close to each other.

The SHA.DIF.14 models the SV for the last 14 ka, being the longest series of DM (Dipolar Moment) of geomagnetic field among the models we have studied. In Fig. 15 the DM series of this model and the averaged series of dipolar moment generated and calculated by domino model (Eq. (8)) are shown. In this case, the match between two curves is the worst one (RMSD = 52.5%) In Fig. 16a and b, the respective PSDs are shown. Differently from the other models, the PSD of SHA.DIF.14 model has a three-slope shape, all of them being negative where the middle slope has the smallest coefficient (largest in module). The averaged time series generated by domino model shows a strikingly similar qualitative behavior and, quantitatively, the slope coefficients are close to that of the SV model.

It would be very interesting to investigate if this latter set of parameters is appropriate to model not only the SV but also the reversals. We ran the domino model with the same initial conditions as that of SHA.DIF.14 model for a period of 100,000 years starting from 14,000 BP (beginning of SHA.DIF.14 model). The mean time series of ADM, after de-noising small oscillations, is shown in the Fig. 17. As it can be seen, one can find a true reversal (according to our criterion) pointed with a black arrow after about 75,000 from the present time. This reversal seems to be anticipated by a long period of low value of the dipolar moment. So we think that the set of parameters used to model the relatively short time series of SV, can be also used for longer series, and to eventually produce a reversal.

6. Discussions and conclusions

Understanding the physical mechanisms which explain the full (whole) timescales changes of the geomagnetic field remains challenging. Not pretending to enlighten such mechanisms completely, we tried to elucidate some apparently stochastic aspects of these changes. Aiming this, we used the "domino" model versions ("minimal" model, "standard" model and "mean field" model) to generate numerous time series of axial dipolar moment (magnetization). These models considered two main interactions of elementary dipolar elements: the forced orientation to a common axial rotation and the interaction between dipolar elements (neighbor spins or all pairs of spins) producing the tendency of different orientations of elementary dipoles. Other secondary interaction (friction, random forcing) are added to the "standard" and "mean field" model. All such "domino" models elucidate the influence of casual and collective interactions on the generation of long term and short term changes of the dipolar geomagnetic field.

When we used the "standard" model to generate axial dipolar moment (magnetization) series we confirmed most of the results of Mori et al. (2013) regarding the reversals of magnetization. The differences between our results and their results, such as the dependence of *mean chron length or mtr* from the number of macrospins, or the PSD of the magnetization series, can be explained by the different platforms used to implement calculations (numerical integrations) in order to generate magnetization series.

We concluded that the "mean field" model is more appropriate version to match both long and short ranges of the observed dipolar geomagnetic field changes. We have used this model not only to simulate reversals, but also to generate time series of ADM (magnetization) or DM (dipolar moment). For an appropriate set of model parameter values, these series are well matched with the time series of ADM provided by CALS7k.2 model and CALS10k.1b model and with time series of AM provided by SHA.DIF.14 model. Especially the generated series have almost the same statistical behavior as the observed SV of the dipolar field. But, we do not claim that these series reproduces all details of the observed secular variation. The sets of parameters of domino model are the same for all of the SV models used to compare with. Even, not claiming that these values of parameters are the best ones, we noticed a coherence of our results, as the longer time series corresponding to CALS10k.1b model has the same statistical behavior as the shorter time series corresponding to CALS7k.2 model in the overlapping time intervals. We stress the fact that our study is empirical. We ran the algorithms of the "domino" model using many combinations of the values of the model's independent parameters by choosing large interval of γ, λ and κ values and a small value of ε, enough to prevent quick reversals but not too much because it would make the magnetization to saturate very fast. Even the chosen set of parameter values is not unique, we can indicate some limits of these parameter values enabling to generate series of the dipolar moment that are statistically the same as dipolar geomagnetic series provided by the models constructed on the basis of paleomagnetic data. We noticed that the longer the series generated by these models, i.e. the more in the past it goes, the greater are the differences between these series and respective series generated by the "domino" model.

The same set of parameters used by "domino" model to match the SV of the dipolar geomagnetic field provided by the considered models is also used to generate longer series of ADM than these series. We found that such longer series also well approaches to a long series with polarity reversals. Further, the averaged series shows a true reversal (according to our criterion) after about 75,000 years from now and that this reversal persists with a long period of low values of the dipolar moment. We cannot consider this as the exact prediction of a reversal, but we can say this is probably the behavior of the dipolar geomagnetic field in the near future.

Acknowledgements

We would like to thank the unknown referees for their important comments that improved the work significantly.

References

Amit, H., Leonhardt, R., Wicht, J., 2010. Polarity reversals from paleomagnetic observations and numerical dynamo simulations. Space Sci. Rev. 155, 293–335.

Aubert, J., Aurnou, J., Wicht, J., 2008. The magnetic structure of convection-driven numerical dynamos. Geophys. J. Int. 172, 945–956.

Aubert, J., Tarduno, J.A., Johnson, C.L., 2010. Observations and models of the long-term evolution of earth's magnetic field. Space Sci. Rev. http://dx.doi.org/10.1007/s11214-010-9684-5.

Biggin, A.J., van Hinsbergen, D.J.J., Langereis, C.G., Straathof, G.B., Deenen, M.H.L., 2008. Geomagnetic secular variation in the Cretaceous normal superchron and in the Jurassic. Phys. Earth Planet. Inter. 169, 3–19. http://dx.doi.org/10.1016/j.pepi.2008.07.004.

Biggin, A.J., Steinberger, B., Aubert, J., Suttie, N., Holme, R., Torsvik, T.H., van der Meer, D.G., van Hinsbergen, D.J.J., 2012. Possible links between long-term geomagnetic variations and whole-mantle convection processes. Nat. Geosci. 5, 526–533.

Busse, F.H., 1975. A model of the geodynamo. Geophys. J. Roy. Astron. Soc. 42, 437–459.

Channell, J.E.T., Xuna, C., Hodell, D.A., 2009. Stacking paleointensity and oxygen isotope data for the last 1.5 Myr (PISO-1500). Earth Planet. Sci. Lett. 283, 14–23.
Cox, A., 1968. Lengths of geomagnetic polarity intervals. J. Geophys. Res. 73 (10), 3247–3260. http://dx.doi.org/10.1029/JB073i010p03247.
Cande, S.C., Kent, D.V., 1995. A new geomagnetic polarity time scale for the late Cretaceous and Cenozoic. J. Geophys. Res. 97, 13917–13951.
Christensen, U.R., Wicht, J., 2007. Numerical Dynamo Simulations, Treatise on Geophysics Vol 8 – Ch8, vol 8. Elsevier.
Constable, C.G., Parker, R.L., 1988. Statistics of the geomagnetic secular variation for the past 5 Ma. J. Geophys. Res. 93, 11569–11582.
Constable, C., 2001. Geomagnetic Reversals: Rates, Timescales, Preferred Paths, Statistical Models and Simulations, The Fluid Mechanics of Astrophysics and Geophysics (Chapter 5). CRC Press.
Davidson, P.A., 2013. Turbulence in rotating, stratified and electrically conducting fluids". Cambridge University Press.
De Santis, A., Qamili, E., Wu, L.X., 2013. Toward a possible next geomagnetic transition? Nat. Hazard. Earth Syst. Sci. 13, 3395–3403.
Dormand, J.R., Prince, P.J., 1980. A family of embedded Runge-Kutta formulae". J. Comput. Appl. Math. 6 (1980), 19–26.
Duka, B., De Santis, A., Mandea, A., Isac, A., Qamili, E., 2012. Geomagnetic jerks characterization via spectral analysis. Solid Earth 3, 131–148.
Finlay, C.C. et al., 2010. International Geomagnetic Reference Field: the eleventh generation. Geophys. J. Int. 183, 1216–1230.
Glaßmeier, K.-H., Soffel, H., Negendank, J., 2009. Geomagnetic Field Variations. Springer-Verlag, Berlin Heidelberg.
Glatzmaier, G.A., Coe, R.S., Hongre, L., Roberts, P.H., 1999. The role of the Earth's mantle in controlling the frequency of geomagnetic reversals. Nature 401, 885–890.
Glatzmaier, G.A., Roberts, P.H., 1995. A three-dimensional self-consistent computer simulation of a geomagnetic field reversal. Nature 377, 203–209.
Glatzmaier, G.A., Roberts, P.H., 1997. Numerical simulations of the geodynamo. Acta Astron. Et Geophys. Uni. Comenianae XIX, 125–143.
Gubbins, D., 1999. The distinction between geomagnetic excursions and reversals. Geophys. J. Int. 137, F1–F3.
Guyodo, Y., Valet, J.-P., 1999. Global changes in intensity of the Earth's magnetic field during the past 800 kyr. Nature 399, 249–252.
Hatakeyama, T., Kono, M., 2002. Geomagnetic field model for the last 5 My: time-averaged field and secular variation. Phys. Earth Planet. Inter. 133, 181–215.
Hejda, P., Reshetnyak, M., 2012. Domino model in geodynamo, arXiv:1209.5314 [physics.flu-dyn].
Heimpel, M.H., Evans, M.E., 2013. Testing the geomagnetic dipole and reversing dynamo models over Earth's cooling history. Phys. Earth Planet. Inter. 224, 124–131. http://dx.doi.org/10.1016/j.pepi.2013.07.007.
Jackson, A., Jonkers, A.R.T., Walker, M.R., 2000. Four centuries of geomagnetic secular variation from historical records. Phil. Trans. R. Soc. Lond. 358, 957–990.
Jacobs, J.A., 1994. Reversals of the Earth's magnetic field. Cambridge University Press.
Johnson, C.L., Constable, C.G., 1997. The time-averaged geomagnetic field: global and regional biases for 0–5 Ma. Geophys. J. Int. 131 (3), 643–666.
Kageyama, A., Sato, T., 1997. Velocity and magnetic field structures in a magnetohydrodynamic dynamo. Phys. Plasmas 4, 1569–1575.
Kono, M., Roberts, P.H., 2002. Recent geodynamo simulations and observations of the geomagnetic Field. Rev. Geophys. 40 (4), 14–53.
Korte, M., Constable, C.G., 2005. Continuous geomagnetic field models for the past 7 millennia: 2 CALS7K. Geochem. Geophys. Geosyst. 6, Q02H16.
Korte, M., Constable, C., Donadini, F., Holme, R., 2011. Reconstructing the Holocene geomagnetic field. Earth Planet. Sci. Lett. 312, 497–505.
Kutzner, C., Christensen, U.R., 2004. Simulated geomagnetic reversals and preferred virtual geomagnetic pole paths. Geophys. J. Int. 157 (3), 1105–1111.
Lhuillier, F., Fournier, A., Hulot, G., Aubert, J., 2011. The geomagnetic secularvariation timescale in observations and numerical dynamo models. Geophys. Res. Lett. 38 (9). http://dx.doi.org/10.1029/2011GL047356.
Lhuillier, F., Gilder, S.A., 2013. Quantifying paleosecular variation: insights from numerical dynamo simulations. Earth Planet. Sci. Lett. 382, 87–97. http://dx.doi.org/10.1016/j.epsl.2013.08.048.
Lhuillier, F., Hulot, G., Gallet, Y., 2013. Statistical properties of reversals and chrons in numerical dynamos and implications for the geodynamo. Phys. Earth Planet. Inter. 220, 19–36.
Lowes, F.J., 1974. Spatial power spectrum of the main geomagnetic field, and extrapolation to the core. Geophys. J. R. Astron. Soc. 36, 717–730.
Lowrie, W., Kent, D.V., 2004. Geomagnetic polarity timescales and reversal frequency regimes. In: Channell, J.E.T., Kent, D.V., Lowrie, W., Meert, J.G. (Eds.), Timescales of the Paleomagnetic Field, vol. 145. AGU, pp. 117–129.
Lund, S., Stoner, J.S., Channell, J.E.T., Acton, G., 2006. A summary of Bruhnes paleomagnetic field variability recorded in ocean drilling Program Cores. Phys. Earth Planet. Inter. 156, 194–204.
Mazaud, A., Laj, C., 1989. Simulation of geomagnetic polarity reversals by a model of interacting dipole sources. Earth Planet. Sci. Lett. 92, 299–306.
Merrill, R.T., McElhinny, M.W., McFadden, P.L., 1996. The Magnetic Field of The Earth: Paleomagnetism, The Core, and The Deep Mantle. Academic Press, San Diego.
Mori, N., Schmitt, D., Ferriz-Mas, A., Wicht, J., Mouri, H., Nakamichi, A., Morikawa, M., 2011. A domino model for geomagnetic field reversals, arXiv:1110.5062 [astro-ph.EP].
Mori, N., Schmitt, D., Wicht, J., Ferriz-Mas, A., Mouri, H., Nakamichi, A., Morikawa, M., 2013. Domino model for geomagnetic field reversals. Phys. Rev. E 87, 012108.
Naidu, P., 1971. Statistical structure of geomagnetic field reversals. J. Geophys. Res. 76 (11), 2649–2662. http://dx.doi.org/10.1029/JB076i011p02649.
Nakamichi, A., Mouri, H., Schmitt, D., Ferriz-Mas, A., Wicht, J., Morikawa, M., 2011. Coupled spin models for magnetic variation of planets and stars, arXiv:1104.5093 [astro-ph.EP].
Olson, P., Amit, H., 2014. Magnetic reversal frequency scaling in dynamos with thermochemical convection. Phys. Earth Planet. Inter. 229, 122–133.
Olson, P.L., Coe, R.S., Driscoll, P.E., Glatzmaier, G.A., Roberts, P.H., 2010. Geodynamo reversal frequency and heterogeneous core-mantle boundary heat flow. Phys. Earth Planet. Inter. 180, 66–79.
Olson, P., Hinnov, L.A., Driscoll, P.E., 2014. Nonrandom geomagnetic reversal times and geodynamo evolution. Earth Planet. Sci. Lett. 388, 9–17.
Pavón-Carrasco, F.J., Osete, M.L., Torta, J.M., De Santis, A., 2014. A geomagnetic field model for the Holocene based on archaeomagnetic and lava flow data. Earth Planet. Sci. Lett. 388, 98–109.
Press, W.H., Rybicki, G.B., 1989. Fast algorithm for spectral analysis for unevenly sampled data. Astrophys. J. 338, 277–280.
Press, W.H., Teukolsky, S.A., Vetterling, W.T., Flannery, B.P., 1996. Fortran Numerical Recipes. Cambridge Univeristy Press, p. 5.
Roberts, P.H., Glatzmaier, G.A., 2000. Geodynamo theory and simulations. Rev. Mod. Phys. 72, 1081–1124.
Roberts, A., 2008. Geomagnetic excursions: knowns and unknowns. Geophys. Res. Lett. 35, L17307.
Ryan, D.A., Sarson, G.R., 2007. Are geomagnetic field reversals controlled by turbulence within the Earth's core? Geophys. Res. Lett. 34, L02307.
Sagnotti, L., Scardia, G., Giaccio, B., Liddicoat, J.C., Nomade, S., Renne, P.R., Sprain, C.J., 2014. Extremely rapid directional change during Matuyama-Brunhes geomagnetic polarity reversal. Geophys. J. Int. 199, 1110–1124.
Vandamme, D., 1994. A new method to determine paleosecular variation. Phys. Earth Planet. Inter. 85 (1–2), 131–142.
Valet, J.P., Plenier, G., Herrero-Bervera, E., 2008. Geomagnetic excursions reflect an aborted polarity state. Earth Planet. Sci. Lett. 274, 472–478. http://dx.doi.org/10.1016/j.epsl.2008.07.056.
Valet, J., Meynadier, J., Guyodo, Y., 2005. Geomagnetic dipole strength and reversal rate over the past two million years. Nature 435 (7043), 802–805. http://dx.doi.org/10.1038/nature03674 R. v.
Verosub, K., 1977. Geomagnetic excursions and their paleomagnetic record. Rev. Geophys. Space Phys. 15, 145–155.
Wicht, J., Stellmach, S., Harder, H., 2009. Numerical models of the geodynamo: from fundamental cartesian models to 3D simulations of field reversals. In: Glassmeier, K.-H., Soffel, H., Negendank, J.F.W. (Eds.), Geomagnetic Field Variations. Springer, pp. 107–158.